Global estimate of submarine groundwater discharge based on an observationally constrained radium isotope model

Eun Young Kwon[1], Guebuem Kim[1], Francois Primeau[2], Willard S. Moore[3], Hyung-Mi Cho[1], Timothy DeVries[4], Jorge L. Sarmiento[5], Matthew A. Charette[6], and Yang-Ki Cho[1]

[1]Research Institute of Oceanography/School of Earth and Environmental Sciences (BK21), Seoul National University, Seoul, South Korea, [2]Earth System Science, University of California, Irvine, California, USA, [3]Department of Earth and Ocean Sciences, University of South Carolina, Columbia, USA, [4]Department of Geography, University of California, Santa Barbara, California, USA, [5]Atmospheric and Oceanic Sciences, Princeton University, Princeton, New Jersey, USA, [6]Woods Hole Oceanographic Institution, Woods Hole, Massachusetts, USA

Abstract Along the continental margins, rivers and submarine groundwater supply nutrients, trace elements, and radionuclides to the coastal ocean, supporting coastal ecosystems and, increasingly, causing harmful algal blooms and eutrophication. While the global magnitude of gauged riverine water discharge is well known, the magnitude of submarine groundwater discharge (SGD) is poorly constrained. Using an inverse model combined with a global compilation of ^{228}Ra observations, we show that the SGD integrated over the Atlantic and Indo-Pacific Oceans between 60°S and 70°N is $(12 \pm 3) \times 10^{13}$ m^3 yr^{-1}, which is 3 to 4 times greater than the freshwater fluxes into the oceans by rivers. Unlike the rivers, where more than half of the total flux is discharged into the Atlantic, about 70% of SGD flows into the Indo-Pacific Oceans. We suggest that SGD is the dominant pathway for dissolved terrestrial materials to the global ocean, and this necessitates revisions for the budgets of chemical elements including carbon.

1. Introduction

The chemical composition of the global ocean is primarily determined by a balance between solute inputs from land and burial into deep ocean sediments [*Broecker and Peng*, 1982; *Berner and Berner*, 1987; *Sarmiento and Gruber*, 2006]. Imbalances between oceanic elemental sources and sinks have driven changes in global biogeochemical cycles, including glacial/interglacial changes in the global carbon cycle [*Toggweiler*, 1999]. Traditionally, rivers have been thought to be the main pathway for input of terrestrial chemical elements into the global ocean. However, accumulating evidence has shown that Submarine Groundwater Discharge (SGD) plays a significant role in determining the biogeochemical properties of some coastal regions [e.g., *Taniguchi et al.*, 2002; *Moore*, 2010; *Lee et al.*, 2010] as well as an ocean basin [*Moore et al.*, 2008]. SGD consists mostly of seawater that invades coastal aquifers, mixes with a small fraction of meteoric water, and then flows back to the ocean [*Burnett et al.*, 2003]. Due to chemical and biological reactions in the coastal aquifer, SGD is enriched with trace elements, rare earth elements, nutrients, and dissolved inorganic and organic carbon [*Charette and Sholkovitz*, 2006; *Moore*, 2010; *Kim and Swarzenski*, 2011; *Kim and Kim*, 2014]. Despite its potential importance in understanding global biogeochemical cycles, a lack of direct measurements has made it difficult to estimate SGD at a global scale. This hampers our understanding of a critical component of global biogeochemical cycles —the exchange of chemical elements between terrestrial and marine environments.

SGD is highly heterogeneous, and direct measurements are limited in their spatial coverage; hence, a great uncertainty arises from the need to extrapolate sparse measurements to the global ocean [*Knee and Paytan*, 2011; *Taniguchi et al.*, 2002, 2009]. An indirect method of estimating SGD based on ^{226}Ra (half-life: 1600 years), enriched in groundwater relative to seawater and rivers, has been applied to local scales such as the South Atlantic Bight [*Moore*, 1996] and the Yellow Sea [*Kim et al.*, 2005]. More recently, ^{228}Ra (half-life: 5.75 years) has been used for estimating SGD to the Atlantic Ocean [*Moore et al.*, 2008]. The dominant sink for ^{228}Ra in the open ocean is radioactive decay. At steady state, the removal rate of ^{228}Ra by radioactive decay should be equal to the supply rate from land [*Moore et al.*, 2008]. By subtracting contributions from wind-blown dust, diffusive fluxes from coastal sediments, and rivers, and then using the end-member concentrations of the ^{228}Ra flux,
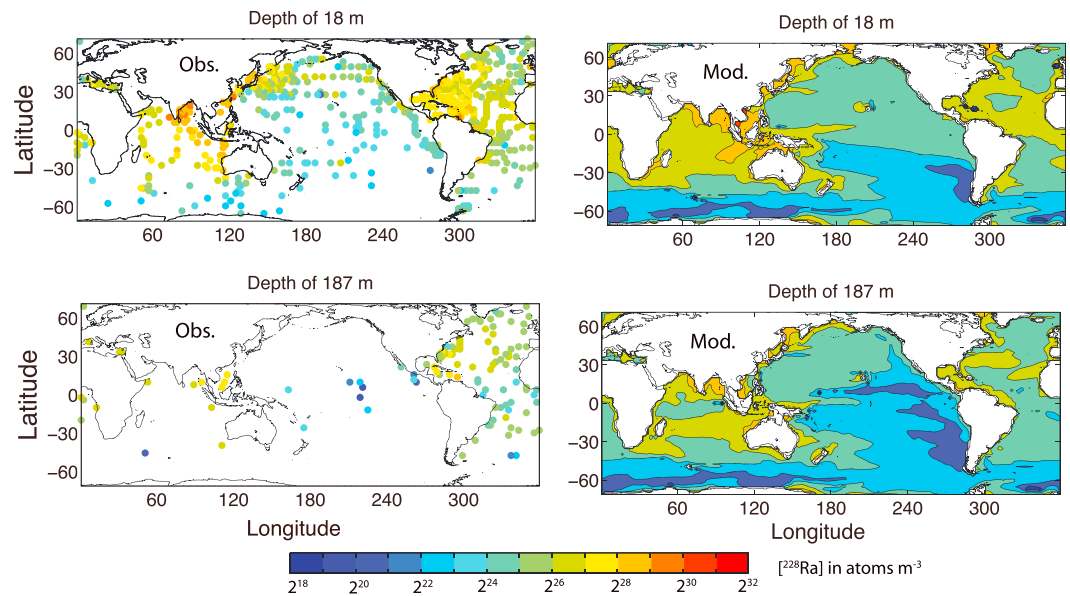
Figure 1. The distributions of ^{228}Ra in the global ocean between 60°S and 70°N. Two representative model depths of 18 and 187 m are chosen to show the distributions at the surface and within the thermocline. Observations are shown with dots on the left panels. The observations are taken from a depth range of ±50 m. Simulated ^{228}Ra concentrations are shown in color shading on the right panels. Unit is in atoms m^{-3} with a conversion factor of 1 dpm = 4.36 × 10^6 atoms. Note that the color scale is made in a log scale with a base of 2 (i.e., log$_2$[^{228}Ra]) to increase the visual effect.

Moore et al. [2008] estimated the SGD flux into the Atlantic basin to be 0.8 to 1.6 times greater than the Atlantic freshwater flux from rivers.

Although the indirect method based on a ^{228}Ra budget analysis has been successfully applied to the Atlantic Ocean [*Moore et al.*, 2008], it is problematic to apply the same method to the global ocean where ^{228}Ra observations are extremely sparse below the surface (Figure 1). Therefore, to obtain the upper ocean inventory of ^{228}Ra, surface ^{228}Ra observations need to be extrapolated while accounting for the source distributions and ocean circulation. To address this issue, we developed a ^{228}Ra inverse model based on a data-constrained global ocean circulation model of *DeVries and Primeau* [2011], and combined the model with a compilation of ^{228}Ra observations. This novel approach allows us to infer the SGD integrated over the global ocean between 60°S and 70°N (hereafter referred to as the global ocean noting that the polar regions are beyond the scope of this study). We will show that the global SGD is 3 to 4 times greater than the freshwater fluxes into the global ocean by rivers, and that the Indo-Pacific Oceans account for about 70% of the total SGD.

This paper is organized as follows. In section 2, we describe the inverse modelling approach. In section 3, we test our method for the Atlantic Ocean to explore any potential biases associated with the sparse observational points of the Indo-Pacific Oceans. In section 4, we present the global estimate of SGD. Section 5 discusses implications of SGD on global biogeochemical cycles.

2. Methods

We take two steps to estimate the SGD. First, we use a ^{228}Ra inverse model to constrain the coastal source of ^{228}Ra. The coastal ^{228}Ra source obtained from the first step includes the contributions from rivers, coastal sediments, and SGD. Therefore, in the second step, we subtract the river and sediment contributions from the total coastal fluxes of ^{228}Ra to obtain the SGD component of the ^{228}Ra fluxes. This section describes the method by which we estimate the integrated coastal source of ^{228}Ra using the inverse model. The second step, which is performed outside the model, is presented in section 4 along with the results.

2.1. The ^{228}Ra Inverse Model

The circulation model is a modified version of the data-constrained global ocean circulation model described in *DeVries and Primeau* [2011] and is taken from *DeVries* [2014]. The ocean circulation field is constrained by

observed temperature, salinity, radiocarbon, Chlorofluorocarbon-11, sea surface height, and air-sea exchange of heat and freshwater. The model has a horizontal resolution of $2° \times 2°$ and a vertical resolution ranging from about 40 m near the surface to 600 m near the bottom. Although this model has a global domain, our focus area only includes the global ocean between 60°S and 70°N due to insufficient ^{228}Ra observations from the polar regions. In this study, we also exclude deep waters influenced by benthic sediment sources of ^{228}Ra, focusing on the coastal source only.

The governing equation for ^{228}Ra is

$$\frac{\partial [Ra]}{\partial t} = -U\nabla[Ra] + \nabla(K\nabla[Ra]) - \lambda[Ra] + S_0 + S(p),$$ (1)

where $[Ra]$ is ^{228}Ra concentration (atoms m^{-3}); note that $[Ra]$ can also be reported in activity units, disintegrations per minute (dpm) m^{-3}. One dpm corresponds to 4.36×10^6 atoms; the first and second terms on the right-hand side represent ocean advection and mixing, respectively; λ is the radioactive decay constant (0.12 yr^{-1}); and S_0 is an atmospheric source due to mineral dust deposition. The atmospheric source of mineral dust deposition and input from solubilization due to desorption are prescribed using a global map of mineral dust deposition [*Mahowald et al.*, 2005] and a desorption rate of 8.6×10^6 atoms g^{-1} [*Moore et al.*, 2008]. $S(p)$ is the combined coastal source from sediments, rivers, and SGD.

The coastal source $S(p)$ is defined as ^{228}Ra fluxes from the ocean grid boxes adjacent to terrestrial grid boxes shallower than ~200 m (a precise depth of 217 m in the model). This depth limit is chosen because it gives the minimum value of the misfit between the model and observations. By restricting the coastal source to the continental shelf, we assume that the ^{228}Ra contribution from the continental slope to the open ocean is negligible. Indeed, *Taniguchi et al.* [2002] noted that most of aquifers outcrop within the continental shelf. We model only the horizontal variation of the coastal source with a fixed thickness of 217 m by dividing the coastal grid boxes depending on their geographic locations into 20 groups for the Atlantic and 30 groups for the Indo-Pacific Ocean. Thus, p represents 50 discrete source amplitudes to be estimated in the inverse model. This number of groups is chosen so that the coastal sources can be well constrained by available observations.

2.2. Optimization of the Coastal ^{228}Ra Source

The integrated coastal source (i.e., the sum of sediments, rivers, and SGD) is optimized by minimizing the misfit between the model and observation given by

$$C(p) = \frac{1}{\sigma^2} \sum_{i=1}^{N} \left([Ra]_i^{obs} - [Ra]_i^{mod} \right)^2$$ (2)

where σ^2 is the variance of the misfit between the model and the observations; N is the number of observations; $[Ra]^{obs}$ is the observed ^{228}Ra concentration; and $[Ra]^{mod}$ is the simulated ^{228}Ra concentration, which is interpolated onto the locations where the observations are taken. Note that the cost function C is a function of p because simulated ^{228}Ra distributions depend on the coastal source amplitudes p. We obtain an optimized set of the coastal source amplitudes $\hat{p}$ by minimizing the cost function C. One-standard error of $\hat{p}$ is then obtained by assuming a Gaussian distribution of the model-observation differences (see Appendix A).

3. Atlantic Ocean Coastal ^{228}Ra Fluxes

The inverse modeling approach is first tested in the Atlantic Ocean to explore how sampling biases, related to a higher density of measurements near the sea surface, affect the estimates. The integrated coastal source of ^{228}Ra for the Atlantic Ocean, which includes coastal sediments, rivers, and SGD, is estimated to be $(3.1 \pm 0.1) \times 10^{23}$ atoms yr^{-1} with an estimated atmospheric dust contribution of 1.7×10^{21} atoms yr^{-1}. The error bar represents ± one standard deviation of the posterior distribution for the inferred source (Appendix A). The uncertainty includes the combined errors associated with the model and the measurements. An important contributor to the uncertainty arises from the fact that the sparse observations are influenced by high-frequency small-scale fluctuations that are not captured by the steady-state model with a $2° \times 2°$ resolution.

In the case of using a data subset sub-sampled from only the surface layer, the integrated coastal source (i.e., $(3.3 \pm 0.7) \times 10^{23}$ atoms yr^{-1}) is not significantly different from the estimate with all the available data
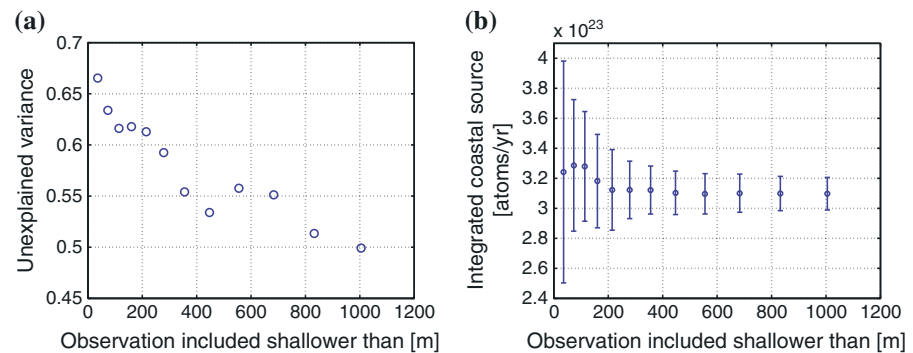
Figure 2. The sensitivity of the optimization to subsampling of observations for the Atlantic Ocean only. (a) The sensitivity of the cost function. The *x* axis shows the depth limit to which the ^{228}Ra observations are sub-sampled to constrain the ^{228}Ra coastal source. (b) The sensitivity of the resulting integrated coastal source. The error bars indicate the ± one standard deviation of the posterior distribution for the estimated source.

(Figure 2). With a reduced error bar, the integrated Atlantic coastal source of $(3.1 \pm 0.1) \times 10^{23}$ atoms yr^{-1} in this study has improved the previous estimate of $(3.5 \pm 0.7) \times 10^{23}$ atoms yr^{-1} made by *Moore et al*. [2008] using a statistical analysis of the same data. This agreement, along with the relative insensitivity of our estimate to the depth distribution of ^{228}Ra observations, provides confidence in applying the inverse modeling approach to the global ocean.

4. An Estimate of SGD to the Global Ocean Between 60°S and 70°N

We use a compilation of previously published data (Table S1 and Figure 1) to constrain the globally integrated coastal source of ^{228}Ra. We exclude ^{228}Ra data greater than one standard deviation (i.e., [^{228}Ra] >140 disintegrations per minute (dpm) m$^{-3} = 6 \times 10^8$ atoms m^{-3}), mostly found in marginal seas (Figure S1). By excluding extremely large point values, we focus our attention on coastal measurements of ^{228}Ra that integrate coastal sources and influence the open ocean on large spatial and temporal scales. This data control is necessary as we neglect small-scale physical and biogeochemical processes that are not well represented in our model. The sensitivity of our result to the data control is discussed in Figure S1. After setting the atmospheric wind-blown dust source to be 2.9×10^{21} atoms yr^{-1}, we estimate the globally integrated coastal source, which includes rivers, sediments, and SGD, to be $(9.6 \pm 0.5) \times 10^{23}$ atoms yr^{-1}.

To obtain an estimate of the SGD driven ^{228}Ra fluxes to the global ocean, we then subtract contributions from rivers and coastal sediments from the above globally integrated coastal source of ^{228}Ra. The river contribution is removed following the approach taken in *Moore et al*. [2008]. Using a sediment load to the global ocean of 1.8×10^{16} g yr^{-1} [*Milliman*, 2001] and a desorption rate of 8.6×10^6 atoms g^{-1}, the ^{228}Ra flux due to riverine sediment load becomes 1.5×10^{23} atoms yr^{-1}. We also use the average dissolved ^{228}Ra of 1.3×10^8 atoms m^{-3} and the total riverine water fluxes of 3.5×10^{13} m^3 yr^{-1} [*Milliman*, 2001; *Dai and Trenberth*, 2002] to account for the dissolved ^{228}Ra fluxes by rivers of 0.05×10^{23} atoms yr^{-1}. Taken together the total riverine input is estimated to be $(1.6 \pm 0.5) \times 10^{23}$ atoms yr^{-1}, assuming a 30% uncertainty. We also follow *Moore et al*. [2008] to estimate the ^{228}Ra source from coastal sediments. Using the bathymetry data [*Sindhu et al*., 2007] re-gridded onto the model domain, the global shelf area between 60°S and 70°N shallower than 217 m is determined to be 1.5×10^{13} m^2. We assume that 30% of the shelf area is composed of fine-grained sediments and 70% is composed of coarse-grained sediments [*Emery*, 1968] with fluxes of $(50 \pm 25) \times 10^9$ atoms m^{-2} yr^{-1} and $(1.0 \pm 0.5) \times 10^9$ atoms m^{-2} yr^{-1}, respectively [*Moore et al*., 2008]. Thus, the contribution from coastal sediments is calculated to be $(2.4 \pm 1.2) \times 10^{23}$ atoms yr^{-1}. Considering the contributions from rivers and sediments together, we obtain by difference a global SGD ^{228}Ra flux of $(5.6 \pm 1.4) \times 10^{23}$ atoms yr^{-1}. The Indian, North Atlantic, and North Pacific Oceans are the dominant source regions for the global ^{228}Ra inputs with almost equal strengths (Figure 3).

Although the SGD ^{228}Ra flux is the dominant source for the upper ocean ^{228}Ra inventory (Figure 3), it remains to be seen whether SGD is a major pathway for the exchange of water between the continents and the
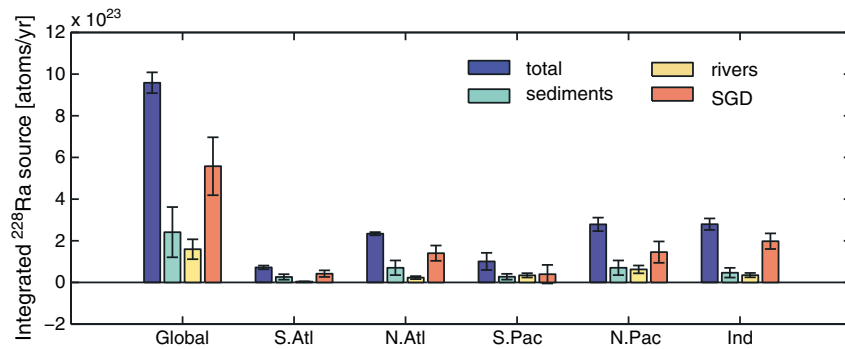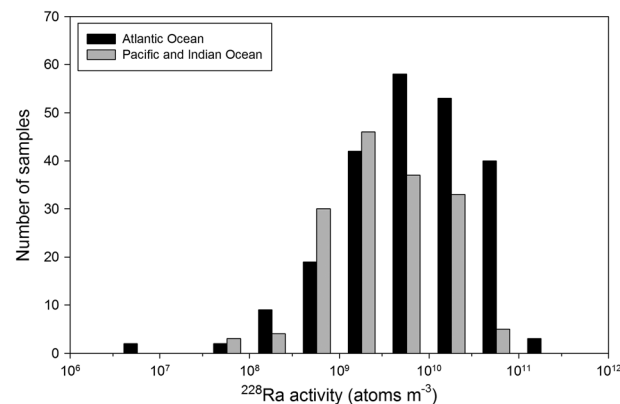
Figure 3. Integrated ^{228}Ra coastal fluxes. The coastal fluxes are divided into the contributions from coastal sediments, rivers, and submarine groundwater discharge (SGD). The (left) global estimates are divided into five basins—the South Atlantic, North Atlantic, South Pacific, North Pacific, and Indian Oceans.

oceans. For large temporal and spatial scales relevant to the open ocean, SGD fluxes can be obtained by dividing the SGD ^{228}Ra flux by the ^{228}Ra end-member concentrations of the SGD. To estimate the globally averaged ^{228}Ra end-member concentrations of the SGD, we combine the Indo-Pacific SGD ^{228}Ra data with those reported by *Moore et al.* [2008] (Figure 4 and Table S2). To account for the skewness, we assume a lognormal distribution of SGD ^{228}Ra concentrations. The resulting estimate of $(4.3–5.0) \times 10^9$ atoms m^{-3}, which is slightly lower than $(5.55–6.94) \times 10^9$ atoms m^{-3} for the Atlantic Ocean only [*Moore et al.*, 2008], is then used to infer an SGD flux of $(12 \pm 3) \times 10^{13}$ m^3 yr^{-1} into the Atlantic and Indo-Pacific Oceans. We speculate that the average activities of ^{228}Ra in SGD are likely to be lower in high seepage rate regions due to less ingrowth time of ^{228}Ra from its parent ^{232}Th in sediments and rocks. If this is the case, then the global SGD calculated here might be a lower-limit estimate.

5. Discussions

We have used a numerical model combined with ^{228}Ra observations to estimate the SGD flux into the global ocean between 60°S and 70°N. The ^{228}Ra tracer based estimate of $(12 \pm 3) \times 10^{13}$ m^3 yr^{-1} roughly agrees with a global extrapolation of actual seepage measurements $[(6.1–12.8) \times 10^{13}$ m^3 yr^{-1}; *Taniguchi et al.*, 2009]. When compared with a freshwater discharge of $(3.0–3.5) \times 10^{13}$ m^3 yr^{-1} by rivers [*Milliman*, 2001; *Dai and Trenberth*, 2002], our estimated SGD is 3 to 4 times greater than the river water fluxes to the Atlantic and Indo-Pacific Oceans. The estimated SGD is significantly higher than the freshwater component of SGD constrained by the global hydrological cycle (i.e., 0.01–10% of total river flow) [*Taniguchi et al.*, 2002]; this is consistent with many local or regional studies reporting that marine salty groundwater is a dominant source (>90%) of SGD [*Burnett et al.*, 2003; *Kim et al.*, 2003; *Taniguchi et al.*, 2006]. Our study is also in accordance with an early study of *Riedl et al.* [1972] who suggested an "intertidal pump" magnitude of 9.6×10^{13} m^3 yr^{-1}, which is close to our estimate. This seawater circulation portion of SGD is important for oxygenating benthic marine ecosystems and is a contributor to saltwater intrusion in coastal aquifers [*Reilly and Goodman*, 1987]. The mixture of fresh and salty groundwaters flowing back to the surrounding seas has been biogeochemically modulated within the coastal aquifers, transferring terrestrial materials to the

Figure 4. The distribution of ^{228}Ra in groundwater samples from the Pacific and Indian Oceans using the compiled data shown in Supporting Information Table S2 in comparison with those from the Atlantic Ocean [*Moore et al.*, 2008].

surrounding seas [*Charette and Sholkovitz*, 2006]. Our estimate of the SGD flux into the global ocean suggests that the land-ocean interaction is far more dynamic than previously believed, and that SGD may constitute the largest terrestrial source for certain oceanic chemical species including nutrients, carbon, and trace metals.

The globally integrated estimate of SGD reported here will aid in understanding the SGD-driven fluxes of chemical elements to the global ocean. This can be achieved through extensive measurements of the biogeochemical properties of coastal groundwaters flowing into the ocean as seeps and springs. Additionally, more extensive measurements of ^{228}Ra end-member concentrations will allow us to resolve the spatial distributions of SGD, helping us identify regions of enhanced SGD fluxes. Using the previously suggested SGD for the Atlantic Ocean of $\sim 3 \times 10^{13}\,\mathrm{m^3\,yr^{-1}}$ [*Moore et al.*, 2008], this study suggests that about 70% of SGD occurs in the Indo-Pacific Oceans. The SGD distribution is somewhat different from the riverine discharge in that less than a half of global river waters are discharged into the Indo-Pacific Oceans [*Milliman*, 2001]. The global distribution of SGD implies that the Indo-Pacific Oceans may be more susceptible to natural and anthropogenic influences that originate from coastal aquifers. On longer timescales with fluctuating sea levels, the land-ocean dynamics may have been different from the present-day ocean. This may have important implications for the global budgets of some major elements including carbon during glacial-interglacial transitions. This study provides an important step toward quantifying the global land-ocean exchange of natural and anthropogenic chemical species, with implications on pollution, biogeochemical cycles, and ecosystem changes.

Appendix A

This section describes the method in which we provide the error bars of our estimates. We model the likelihood function with a Gaussian probability distribution for the misfit,

$$\mathrm{prob}\left([Ra]_1^{obs},\,[Ra]_2^{obs},\,\cdots,\,[Ra]_N^{obs}\,\middle|\,p,\,\sigma\right) = \prod_{i=1}^{N}\mathrm{prob}\left([Ra]_i^{obs}\,\middle|\,p,\,\sigma\right) = \frac{1}{\left(\sqrt{2\pi}\sigma\right)^N}\exp\left(-\frac{1}{2\sigma^2}\sum_{i=1}^{N}\left([Ra]_i^{obs}-[Ra]_i^{mod}\right)^2\right). \quad \text{(A1)}$$

Assuming a uniform prior for p and $\log(\sigma)$ (i.e., $\mathrm{prob}(p,\sigma) \propto 1/\sigma$), we obtain the posterior probability function for p from Bayes' Theorem as the product of the prior and the likelihood:

$$\mathrm{prob}\left(p,\,\sigma\,\middle|\,[Ra]_1^{obs},\,[Ra]_2^{obs},\,\cdots,\,[Ra]_N^{obs}\right) \propto \frac{1}{\sigma^{N+1}}\exp\left(-\frac{1}{2\sigma^2}\sum_{i=1}^{N}\left([Ra]_i^{obs}-[Ra]_i^{mod}\right)^2\right). \quad \text{(A2)}$$

The most probable value of p (denoted as $\hat{p}$) is obtained by minimizing $C(p)$. The most probable value of σ is obtained by setting the derivative of the log of the posterior with respect to σ equal to zero at $p=\hat{p}$, which gives

$$\hat{\sigma}^2 = \frac{\sum_{i=1}^{N}\left([Ra]_i^{obs}-[Ra]_i^{mod}\right)^2}{N+1}. \quad \text{(A3)}$$

To obtain the error bars of p, we approximate the posterior probability with a Gaussian distribution. To this end, we expand the log of the posterior, i.e.,

$$L(p) = \mathrm{Log}\left(\mathrm{prob}\left(p,\,\sigma\,\middle|\,[Ra]_1^{obs},\,[Ra]_2^{obs},\,\cdots,\,[Ra]_N^{obs}\right)\right)$$

in a Taylor series, and truncate at second order to obtain

$$L(p) = L(\hat{p}) + \frac{1}{2}(p-\hat{p})^T\left[\nabla_{pp}L(p)\right]_{p=\hat{p}}(p-\hat{p}). \quad \text{(A4)}$$

Note that $\nabla_p L(p) = 0$ at $p=\hat{p}$. Exponentiating equation (A4), we obtain a Gaussian function and can identify the inverse of the posterior covariance matrix with

$$H = \frac{1}{2\hat{\sigma}^2}\left(\nabla_{pp}\sum_{i=1}^{N}\left([Ra]_i^{obs}-[Ra]_i^{mod}\right)^2\middle|_{p=\hat{p}}\right). \quad \text{(A5)}$$

The error bars for the individual source amplitudes can be obtained from the posterior covariance matrix H^{-1}. The best estimate for the integrated coastal source is determined by integrating $S(\hat{p})$ over the domain of interest. The uncertainty of the estimate is then obtained by propagating the error bars for $\hat{p}$ to the integrated coastal source, taking into account the error covariance among the different source amplitudes.

References

Berner, E. K., and R. A. Berner (1987), *The Global Water Cycle*, 397 pp., Prentice Hall, N. J.

Broecker, W. S., and T.-H. Peng (1982), *Tracers in the Sea*, Lamont-Doherty Geological Observatory, Columbia Univ., New York.

Burnett, W. C., H. Bokuniewicz, M. Huettel, W. S. Moore, and M. Taniguchi (2003), Groundwater and pore water inputs to the coastal zone, *Biogeochemistry*, *66*, 3–33.

Charette, M. A., and E. R. Sholkovitz (2006), Trace element cycling in a subterranean estuary: Part 2. Geochemistry of the pore water, *Geochim. Cosmochim. Acta*, *70*, 811–826.

Dai, A., and K. E. Trenberth (2002), Estimates of freshwater discharge from continents: Latitudinal and seasonal variations, *J. Hydrometeorol.*, *3*, 660–87.

DeVries, T. (2014), The oceanic anthropogenic CO_2 sink: Storage, air-sea fluxes, and transports over the industrial era, *Global Biogeochem. Cycles*, *28*, 631–647, doi:10.1002/2013GB004739.

DeVries, T., and F. Primeau (2011), Dynamically and observationally constrained estimates of water-mass distributions and ages in the global ocean, *J. Phys. Oceanogr.*, *41*, 2381–2401.

Emery, K. O. (1968), Relict sediments on continental shelves of the world, *Bull. Am. Assoc. Petrol. Geol.*, *52*, 445–464.

Kim, G., and P. W. Swarzenski (2011), Submarine groundwater discharge (SGD) and associated nutrient fluxes to the coastal ocean, in *Carbon and Nutrient Fluxes in Continental Margins a Global Synthesis*, edited by K.-K. Liu et al., pp. 524–538, Springer, Berlin, Heidelberg.

Kim, G., K.-K. Lee, K.-S. Park, D.-W. Hwang, and H.-S. Yang (2003), Large submarine groundwater discharge (SGD) from a volcanic island, *Geophys. Res. Lett.*, *30*(21), 2098, doi:10.1029/2003GL018378.

Kim, G., J. W. Ryu, H. S. Yang, and S. T. Yun (2005), Submarine groundwater discharge (SGD) into the Yellow Sea revealed by [228]Ra and [226]Ra isotopes: Implications for global silicate fluxes, *Earth Planet. Sci. Lett.*, *237*, 156–166.

Kim, I., and G. Kim (2014), Submarine groundwater discharge as a main source of rare earth elements in coastal waters, *Mar. Chem.*, *160*, 11–17.

Knee, K. L., and A. Paytan (2011), Submarine groundwater discharge: A source of nutrients, metals and pollutants to the coastal ocean, in *Treatise on Estuarine and Coastal Science 4*, edited by E. Wolanski and D. S. McLusky, pp. 205–233, Academic Press, Waltham, Mass.

Lee, Y.-W., G. Kim, W.-A. Lim, and D.-W. Hwang (2010), A relationship between submarine groundwater-borne nutrients traced by Ra isotopes and the intensity of dinoflagellate red-tides occurring in the southern sea of Korea, *Limnol. Oceanogr.*, *55*, 1–10.

Mahowald, N. M., A. R. Baker, G. Bergametti, N. Brooks, R. A. Duce, T. D. Jickells, N. Kubilay, J. M. Prospero, and I. Tegen (2005), Atmospheric global dust cycle and iron inputs to the ocean, *Global Biogeochem. Cycles*, *19*, GB4025, doi:10.1029/2004GB002402.

Milliman, J. D. (2001), River inputs, in *Encyclopedia of Ocean Sciences*, edited by J. H. Steele, S. A. Thorpe, and K. K. Turekian, pp. 2419–2427, Academic Press, doi:10.1006/rwos.2001.0074.

Moore, W. S. (1996), Large groundwater inputs to coastal waters revealed by [226]Ra enrichments, *Nature*, *380*, 612–614.

Moore, W. S. (2010), The effect of submarine groundwater discharge on the ocean, *Annu. Rev. Mar. Sci.*, *2*, 59–88.

Moore, W. S., J. L. Sarmiento, and R. M. Key (2008), Submarine groundwater discharge revealed by [228]Ra distribution in the upper Atlantic Ocean, *Nat. Geosci.*, *1*, 309–311.

Reilly, T. E., and A. S. Goodman (1987), Analysis of saltwater upcoming beneath a pumping well, *J. Hydrol.*, *89*, 169–204.

Riedl, R., N. Huang, and R. Machan (1972), The subtidal pump: A mechanism of interstitial water exchange by wave action, *Mar. Biol.*, *13*, 210–221.

Sarmiento, J. L., and N. Gruber (2006), *Ocean Biogeochemical Dynamics*, Princeton Univ. Press, Princeton, N. J.

Sindhu, B., I. Suresh, A. S. Unnikrishnan, N. V. Bhatkar, S. Neetu, and G. S. Michael (2007), Improved bathymetric datasets for the shallow water regions in the Indian Ocean, *J. Earth Syst. Sci.*, *116*, 261–274.

Taniguchi, M., W. C. Burnett, J. E. Cable, and J. V. Turner (2002), Investigation of submarine groundwater discharge, *Hydrol. Process.*, *16*, 2115–2129.

Taniguchi, M., T. Ishitobi, and J. Shimada (2006), Dynamics of submarine groundwater discharge and freshwater-seawater interface, *J. Geophys. Res.*, *111*, C01008, doi:10.1029/2005JC002924.

Taniguchi, M., T. Ishitobi, and W. C. Burnett (2009), Global assessment of submarine groundwater discharge, in *From Headwaters to the Ocean: Hydrological Change and Watershed Management*, edited by M. Taniguchi et al., pp. 613–617, Taylor & Francis, London.

Toggweiler, J. R. (1999), Variation of atmospheric CO_2 by ventilation of the ocean's deepest water, *Paleoceanography*, *14*, 571–588, doi:10.1029/1999PA900033.